Use of magnetization density fluctuation spectra to estimate the electrical resistivity in $YCo_2$



2000 J. Phys.: Condens. Matter 12 5507

(http://iopscience.iop.org/0953-8984/12/25/314)

J. Phys.: Condens. Matter **12** (2000) 5507–5518. Printed in the UK PII: S0953-8984(00)12203-9

# Use of magnetization density fluctuation spectra to estimate the electrical resistivity in $YCo_2$

E Gratz†¶, N Bernhoeft‡, V Paul-Boncour§, H Casalta‖ and A Murani‖

† Institut für Experimentalphysik, Vienna University of Technology, Wiedner Hauptstrasse 8–10, A1040 Wien, Austria
‡ Département de Recherche Fondamentale sur la Matiere Condensé, SPSMS/MSR/CEA/Grenoble, 38054 Grenoble, France
§ CNRS–LCMTR–UPR 209, 94320, Thiais Cédex, France
‖ ILL, Grenoble, France

E-mail: gratz@xphys.tuwien.ac.at

Received 1 March 2000

**Abstract.** Key physical properties of the non-magnetic $RCo_2$ compounds (R = Sc, Y and Lu) suggest that their behaviour is dominated by spin fluctuations. For example, the enhanced linear term in the heat capacity and the $T^2$ increase of the resistivity at low temperatures followed by a pronounced saturation of $\rho$ against $T$ at ambient temperatures have been taken as evidence for this mechanism. We report the measurement of the dynamical spin fluctuation spectrum in polycrystalline $YCo_2$ ($ScCo_2$) samples by a combination of time-of-flight neutron scattering with high energy resolution on the IN5 spectrometer of the Institut Laue–Langevin (ILL) Grenoble with results obtained from the polarized neutron diffractometer D7 (ILL). The low frequency properties of the generalized magnetic susceptibility have been modelled by a single imaginary pole: $\mathrm{Im}[\chi(q,\omega)] = \omega z\chi(q)\Gamma(q)[\omega^2\Gamma(q)^2]^{-1}$ with the static wavevector dependent susceptibility approximated by $\chi(q)^{-1} = \chi_0^{-1} + cq^2$. From the resistivity data we have extracted the spin scattering component and show that it is consistent, using a simple model based on the Boltzmann formalism, with $\mathrm{Im}[\chi(q,\omega)]$ as measured by neutron scattering. In this analysis, the stiffness constant, $c$, which is found to be temperature dependent, appears critical in modelling the saturation of $\rho$ on approaching ambient temperatures.

## 1. Introduction

Among the rare earth (RE)–3d transition metal cubic Laves phases with 1:2 stoichiometry, the magnetism of the 3d partner is most strongly influenced by the magnetic RE sublattice in the Co based compounds (for a review see [1]). Within this $RCo_2$ series $ScCo_2$, $YCo_2$ and $LuCo_2$ are non-magnetic showing, however, behaviour characteristic of exchange enhanced itinerant paramagnetism. In $RCo_2$ compounds with magnetic RE elements the intersublattice f–d exchange field drives the Co sublattice into a ferromagnetic order, with the exception of $TmCo_2$ ($T_C \approx 5$ K) [2], where the f–d exchange interaction does not reach the critical value estimated to be 70 T [3]. Owing to the negative sign of the f–d exchange interaction, compounds with the light RE (Pr, Nd, Sm) are ferromagnetic (i.e. both sublattices are aligned parallel) whereas those with heavy RE (Gd up to Er) are, accordingly, ferrimagnetic.

¶ Corresponding author.

0953-8984/00/255507+12$30.00  

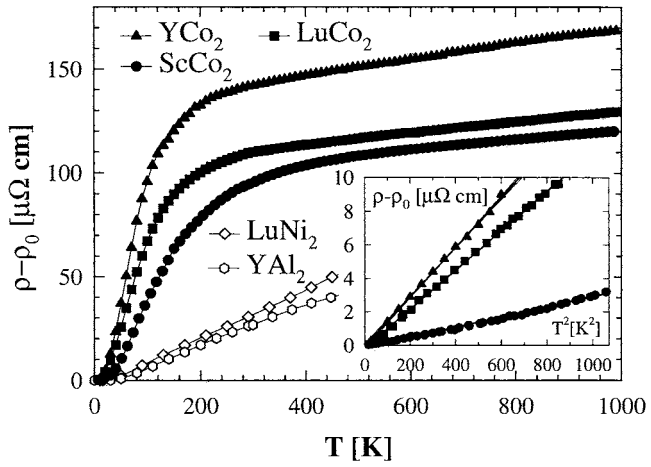


**Figure 1.** The temperature dependence of the electrical resistivity of three spin fluctuation materials $ScCo_2$, $YCo_2$ and $LuCo_2$ is compared with two isostructural non-spin fluctuation compounds $YAl_2$ and $LuNi_2$. The inset shows the low temperature $T^2$ dependence of $\rho(T) - \rho_0$ in the spin fluctuation dominated materials.

The mechanism driving the incipient magnetism in $LuCo_2$, $YCo_2$ and $ScCo_2$ may involve a more subtle interplay (hybridization) of the transition element and rare earth outer d wavefunctions (3d–5d in $LuCo_2$, 3d–4d $YCo_2$ and 3d–3d in $ScCo_2$). In the absence of an internal molecular field this hybridization is expected to be the dominant effect and there are also many reasons to assume that this mechanism is important in the paramagnetic state of the magnetic $RCo_2$ compounds [4]. $YCo_2$, $LuCo_2$ and $ScCo_2$, all exhibit an enhanced, and strongly temperature dependent, bulk susceptibility with a maximum in $\chi$ versus $T$ at 250 K in $YCo_2$, 350 K in $LuCo_2$ and 550 K in $ScCo_2$ [5]. Both thermodynamic and transport properties show marked anomalies in comparison with, for example, the isostructural compounds $YAl_2$ and $LuNi_2$.

The strong temperature dependence of the electrical resistivity of $YCo_2$, $LuCo_2$ and $ScCo_2$, which is characterized by an initial quadratic form followed by a pronounced negative curvature of the $\rho(T)$ curve at elevated temperatures, has been inferred to be due to spin fluctuations (see e.g. [6] and references therein). This outstanding behaviour can best be seen when comparing the $\rho(T)$ curves of these three compounds under consideration with the Ni or Al based Laves phases ($LuNi_2$, $YAl_2$). Figure 1 shows the temperature variation of the resistivity of all these compounds. In the presence of strong spin fluctuation scattering the variation of the resistivity at low temperatures is expected to be of the form $\rho - \rho_0 = AT^2$. The pre-factor $A$ is proportional to the inverse of a characteristic spin fluctuation energy (temperature), i.e. larger $A$ corresponds to a lower spin fluctuation temperature and a stronger spin fluctuation scattering. The inset in figure 1 confirms the anticipated $T^2$ dependence with the following pre-factors: $A(YCo_2) = 0.016\ \mu\Omega$ cm $K^{-2}$, $A(LuCo_2) = 0.012\ \mu\Omega$ cm $K^{-2}$ and $A(ScCo_2) = 0.0043\ \mu\Omega$ cm $K^{-2}$. From this point of view it follows that, among the three compounds under consideration, the influence of the spin fluctuations is weakest in $ScCo_2$. Representation of the $A$ values and corresponding $\gamma_{shc}$ values (linear coefficient of the specific heat) in the so-called Kadowaki–Woods plot [7] is given in figure 2. As can be seen all three $RCo_2$ compounds fit into a linear sequence where other known spin fluctuation systems ($Ni_3Al$, $UAl_2$ etc) are situated. In this letter we report on the first direct evidence for the spin fluctuation spectrum in two of these materials, $YCo_2$ and $ScCo_2$, obtained by

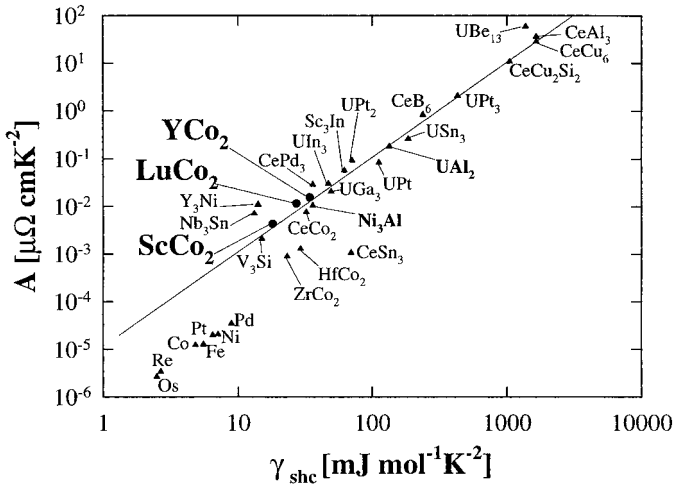


**Figure 2.** The position of $ScCo_2$, $YCo_2$ and $LuCo_2$ in the Kadowaki–Woods plot is shown [7]. $A$ is the pre-factor in the $\rho - \rho_0 = AT^2$ relation ($A(ScCo_2) = 0.0043$, $A(YCo_2) = 0.016$ and $A(LuCo_2) = 0.012$ in units of $\mu\Omega$ cm K$^{-2}$) and $\gamma_{shc}$ is the electronic specific heat coefficient ($\gamma(ScCo_2) = 17$, $\gamma(YCo_2) = 34$, $\gamma(LuCo_2) = 27$ in units of mJ mol$^{-1}$ K$^{-2}$).

a combination of neutron time of flight (spectrometer IN5, ILL, Grenoble) and polarization sensitive spectrometry (spectrometer D7, ILL, Grenoble) and explore the use of these spectra to understand the generic form of the electrical resistivity.

## 2. Experiment

Polycrystalline ingots of $YCo_2$ and $ScCo_2$ were prepared by melting appropriate quantities of the highly purified starting materials in an induction furnace under a protective argon atmosphere and subsequently annealed for periods of typically one week. The use of polycrystalline samples is not only a practical necessity (at this time we are not able to produce sufficiently massive (∼30 gram) single crystals), it also confers advantages since one measures an orientation averaged spectrum of the dynamical magnetization density fluctuations appropriate, for example, to the interpretation of specific heat measurements.

Since one is to characterize a weak magnetic scattering signal, focused in the forward direction, great care must be exercised to eliminate any possibility of spurious (ferromagnetic) phases during sample preparation. To avoid the formation of the ferromagnetic $RCo_3$ phase, the starting composition was shifted out of the ideal stoichiometry RE:Co = 1:2. The optimum procedure to prepare $YCo_2$ and $ScCo_2$ free of the $RCo_3$ ferromagnetic phase consists of a triple remelting of the mixture of RE and Co taken in proportion 1:1.93 and a precise two-step heat treatment; 850 °C for 6 days followed by a one day annealing at 1070 °C. The samples were monitored by powder x-ray diffraction, metallographic optical microscopy, electron microprobe analysis (EMPA) and magnetic susceptibility measurements. EMPA revealed very small inclusions of a phase with composition $YCo_{1.47}$ in a matrix of $YCo_{1.93(1)}$, the inclusions are close to the stoichiometry expected for $Y_2Co_3$ (which is non-magnetic). Since no foreign phase was detected by metallography, its content was estimated to be below 1 vol.%. The measured density of the Y-based samples was $D = 7.18(2)$ g cm$^{-3}$, which corresponds to a composition $YCo_{1.94(1)}$ (for a stoichiometric sample $YCo_2$ the density would be $D = 7.31$ g cm$^{-3}$). X-ray diffraction, using the Rietveld method, showed that the main

phase is cubic C15 with $a = 7.224(1)$ Å. Weak additional reflections, which we assume arose from the inclusion of $YCo_{1.47}$ found in EMPA, were indexed as a cubic phase with $a = 7.978$ Å in agreement with the cell parameter published for $Y_2Co_3$ [8].

The Sc-based samples were also prepared starting with the stoichiometry 1:1.93. Electron-microprobe analysis revealed a composition 1:1.89 whilst the measured density was 6.33(1) g cm$^{-3}$, corresponding to a stoichiometry1:1.92 (for stoichiometric $ScCo_2$ the density should be 6.51 g cm$^{-3}$). X-ray diffraction was refined in the cubic C15-type structure with a cell parameter $a = 6.927$ Å. Following these tests and a preliminary, energy integrated, small angle neutron scattering experiment (spectrometer D22, ILL, Grenoble), the most homogeneous ingots of $YCo_2$ and $ScCo_2$ were selected for the time of flight and polarization analysis experiments.

## 3. Experimental method and results

### *3.1. Electrical resistivity*

For the measurement of the electrical resistivity below room temperature a $^4$He-bath cryostat was used, whilst above room temperature the measurements were made in a furnace at a typical heating rate of 1° min$^{-1}$. The temperature sensor was in both cases a thermocouple (Au(Fe)/chromel in the cryostat and Pt/PtRh in the furnace). In both temperature regions a four-probe dc technique was used and the estimated error in the absolute value of the resistivity is ±5%. The uncertainty is mainly due to the sample geometry and the presence of micro-cracks inside the sample which hinder the determination of the sample cross section. In general it is difficult to separate out the 'spin fluctuation' contribution from the lattice contribution in a bulk measurement such as the electrical resistivity. In the case of $YCo_2$ the intrinsic spin fluctuation contribution to the electrical resistivity has been estimated by the subtraction of 'phonon blank' materials such as $YAl_2$. Using the Matthiessen rule we can determine the temperature variation of the spin fluctuation resistivity, $\rho_{sf}(T)$, in $YCo_2$ firstly by subtracting the residual resistivity, $\rho_0$, from both resistivity curves and the assumption that the temperature variations of the phonon resistivity, $\rho_{ph}(T)$ in $YCo_2$ and $YAl_2$ are the same:

$$\begin{aligned} \rho(YCo_2) - \rho_0(YCo_2) &= \rho_{ph}(T) + \rho_{sf}(T) \\ \rho(YAl_2) - \rho_0(YAl_2) &= \rho_{ph}(T) \end{aligned} \tag{1}$$

it follows:

$$\rho_{sf}(T) = \{\rho(YCo_2) - \rho_0(YCo_2)\} - \{\rho(YAl_2) - \rho_0(YAl_2)\}. \tag{2}$$

This quantity, discussed in detail in section 4.2, is plotted as the open circles in figure 5 (main frame) in the temperature range up to 300 K.

### *3.2. Neutron scattering*

The idea of the linked experiments, IN5 and D7, was to combine the spectral resolution of time of flight energy analysis with a polarization analysis of the energy integrated spectrum. It is necessary to proceed in this manner since the magnetic scattering signal is very weak, typically 5 millibarns sterad$^{-1}$ meV$^{-1}$ atom making it impossible to perform simultaneous energy and polarization analysis. Having established the energy spectrum of the response (IN5) we were able to configure the polarization analysis spectrometer (D7) to perform the required integral over outgoing neutron energies. This then enabled us to isolate the magnetic and non-magnetic scattering cross sections.

### *3.3. Neutron time of flight analysis*

On IN5 data were taken at 1.6 K, 6 K, 120 K, 200 K and 300 K in neutron energy gain scattering. In this manner we were able to use the low temperature spectra as a background since the dynamic scattering falls exponentially to zero for energies above the thermal energy $k_B T$. In order to access small scattering wavevectors in the forward direction, where the response from the dynamic exchange enhanced scattering is anticipated to peak, to have sufficient energy resolution and optimal flux, the IN5 spectrometer was operated at 5 Å incident wavelength. The small angle detector bank was arranged in annuli of 3 cm width centred on the straight through beam position and great care was taken to screen the cryostat and sample housing to reduce the background scattering.

It is found possible to model the data in terms of a quasielastic (within the available energy resolution) Lorentzian line shape consistent with the form expected for that arising from paramagnetic fluctuations in the magnetization density [9]:

$$\frac{\mathrm{d}^2\sigma}{\mathrm{d}\Omega\,\mathrm{d}E} = \frac{\gamma_n^2\alpha}{48\pi^3}\frac{1}{\hbar^2 cN}\frac{|\vec{k}'|}{|\vec{k}|}\langle|B(q,\omega)|^2\rangle \tag{3}$$

where $\gamma_n$ is the neutron gyroscopic factor ($-1.913$), $\alpha = 1/137$ is the fine structure constant, $c$ is the speed of light, $N$ is the number of atoms per unit volume and $\langle|B(q,\omega)|^2\rangle$ is the appropriate power spectrum of field fluctuations defined as the Fourier transform $\vec{r}$ in and $t$ of the unsymmetrized autocorrelation function $\langle\vec{B}(\vec{r}',0)\vec{B}(\vec{r}'+\vec{r},t)\rangle$ in which $\vec{r}'$ is averaged over the volume of the system.

Under our chosen conditions, with low incident neutron energy and small scattering angles to the forward direction, the contamination of the spectra by phonon modes is minimized and the dominant contribution may be expected to be due to spin and associated orbital moment fluctuations, for which, one may write in an isotropic model,

$$\langle|B(q,\omega)|^2\rangle = (4\pi^2)\frac{6\hbar\omega}{\mathrm{e}^{\beta\hbar\omega}-1}\frac{\mathrm{Im}[\chi(q,\omega)]}{\omega}. \tag{4}$$

Here $q = |\vec{k}'-\vec{k}|$ and $\mathrm{Im}[\chi(q,\omega)]$ is the imaginary (absorptive) part of the generalized magnetic susceptibility at energy transfer $\hbar\omega$. When the low frequency properties of the generalized susceptibility can be modelled approximately by a single imaginary pole we may write for sufficiently small $\omega$ and $q$

$$\mathrm{Im}[\chi(q,\omega)] = \omega z\chi(q)\frac{\Gamma(q)}{\omega^2+\Gamma(q)^2}. \tag{5}$$

$\chi(q)$ is the static wavevector dependent susceptibility given by $\chi(q)^{-1} = \chi_0^{-1} + cq^2$ where $\chi_0$ is the bulk susceptibility and $c$ a microscopic stiffness parameter, $z$ a measure of the weight of the low frequency pole and $\Gamma(q)$ the effective relaxation rate [10, 11]. When (5) is employed to model the quasiparticle contribution we find the relaxation rate may be expressed in leading order in $q$ as

$$\Gamma(q) = \gamma q(\chi_0^{-1} + cq^2) \tag{6}$$

where $\gamma$ sets the energy scale of the fluctuations. This form may be physically motivated by consideration of the ballistic transport of Fermionic quasiparticles under an exchange field [9]. For a homogeneous and isotropic Fermi liquid in which spin is conserved overall, $z = 1$ and $\gamma = 2\mu^2 k_F^2/\pi^3$, where $\mu$ is the magnetic moment of the quasiparticles. Since $k_F$ and $\mu$ are not expected to be renormalized by particle and spin conserving interactions, $\gamma$ is here an invariant depending only on bare parameters.

In figure 3 we present the inelastic neutron scattering difference data for $YCo_2$ taken at 120 K, 200 K and 300 K relative to the background at 1.6 K. (The data at 6 K and 1.6 K show

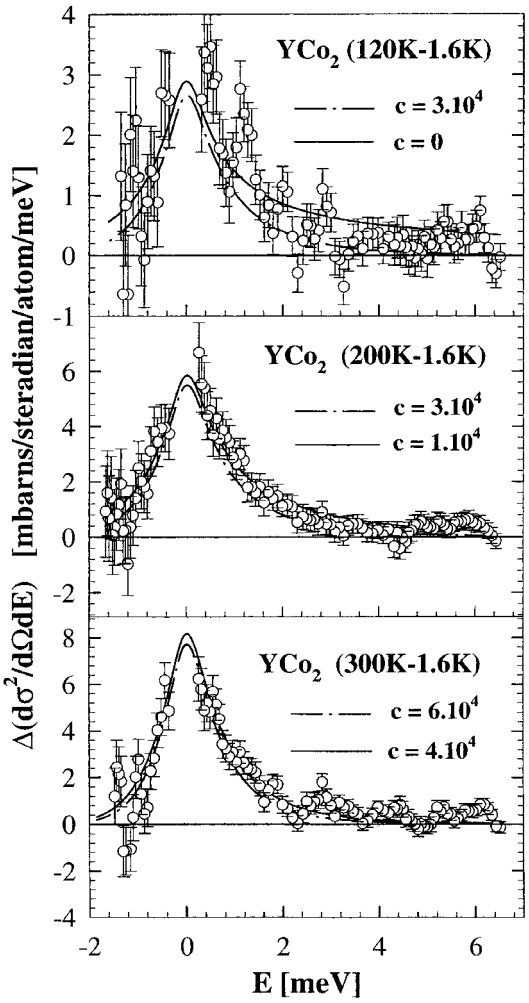


**Figure 3.** Time-of-flight data for $YCo_2$ at 300 K, 200 K and 120 K presented as difference spectra relative to 1.6 K data for scattering angles between 2.8 and 7.44° (average azimuthal angle = 5.13°). The incident neutron wavelength is 5 Å. The solid and broken lines are plotted to give an indication of the sensitivity of the fits to the parameter $c$. In all cases the parameter $\hbar\gamma = 2.6 \times 10^{-3}$ meV Å the bulk susceptibility ($\chi_0$) is taken from that measured [5].

negligible difference.) Using the above formalism for the inelastic cross section, taking the measured bulk magnetic susceptibility and with the data calibrated via a standard vanadium reference sample, we find parameter values of $\gamma$ and $c$ typical for a paramagnetic metal. The interesting observation is that the dynamical fluctuations appear to *soften* on cooling below room temperature. The softening is reflected in a falling value of the microscopic parameter, $c$, used to characterize the spectra. We have put the renormalization into the parameter, $c$, since, as mentioned above, the parameter $\gamma$ is not expected to be affected by particle and spin conserving interactions. In a simple one band model $c$ may be expected to scale like the bulk susceptibility; however, the experimentally inferred softening is much more pronounced than the measured fall of the bulk susceptibility over the given temperature interval [5]. These points will be taken up in the discussion.

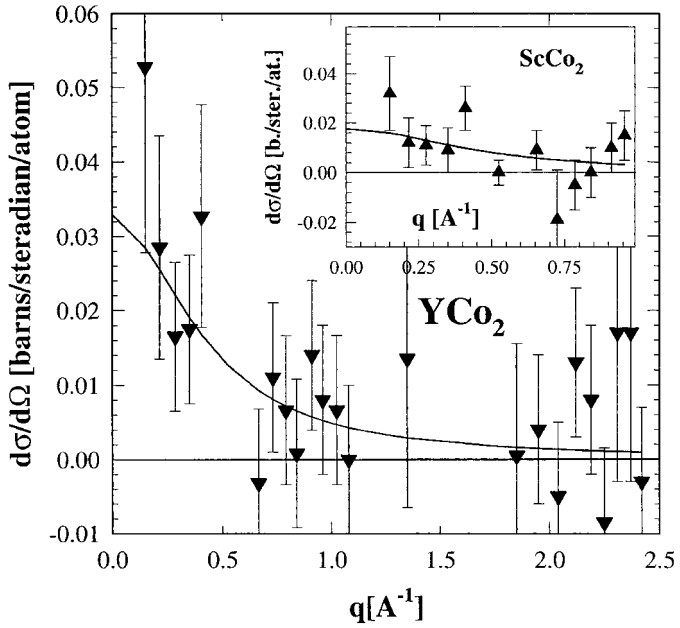


**Figure 4.** Full polarization analysis data taken at 300 K on $YCo_2$ with an incident neutron wavelength 4.8 Å. The energy integrated magnetic cross-section agrees in magnitude and angular dependence with that measured by the difference method on IN5. The estimated value of the parameter $c$ is $6 \times 10^4$ Å$^2$. In the inset we plot data for $ScCo_2$ at 300 K. Fixing the $q = 0$ intercept at the measured bulk susceptibility value [5] we estimate the parameter $c_{ScCo_2} = 1 \times 10^5$ Å$^2$.

### *3.4. Energy integrated polarization analysis*

Polarized neutron measurements were made using the D7 spectrometer at an incident wavelength of 4.8 Å (similar to that used on IN5) over the $q$ range 0.15 Å$^{-1} < q < 2.5$ Å$^{-1}$. Nuclear coherent and spin incoherent scattering were separated from the electronic magnetic scattering by use of the full polarization analysis available on D7. This is achieved by successively projecting the incident neutron polarization onto the orthogonal $x$, $y$ and $z$ axes, right hand convention, with $z$ being defined as the beam direction and $y$ the upward vertical, and recording the spin flipped and non-spin-flipped neutron count rate for each incident polarization. The obtained spectra were corrected for background and multiple scattering effects before being put onto an absolute scale via the nuclear incoherent scattering of the sample (and cross referenced to the nuclear incoherent scattering from a standard vanadium foil). The effect of the beam depolarization was found to be negligible. The samples were held in the same aluminium frame as used on IN5 and similar care in elimination of spurious background signals was taken. Data were taken at temperatures of 1.9 K and 300 K. Results are given, at 300 K, in the main frame of figure 4 for $YCo_2$ and in the inset for $ScCo_2$. On fitting a Lorentzian form for the wavevector dependent susceptibility $\chi(q)^{-1} = \chi_0^{-1} + cq^2$ and using the measured bulk susceptibility $\chi_0$ [5] one obtains an estimate for the parameter $c_{YCo_2} = 6 \pm 1 \times 10^4$ Å$^2$ in $YCo_2$ in accord with the value estimated on IN5; in $ScCo_2$ the parameter is estimated, with less certainty on account of the weaker signal, as $c_{ScCo_2} = 1 \pm 0.3 \times 10^5$ Å$^2$. In this case, D7, in contrast to IN5, the extracted value relies only on the magnitude of the measured bulk susceptibility and not on the absolute calibration of the spectrometer. These data then confirm both the magnetic nature of the cross-section and the

microscopic stiffness parameter ($c$) measured on IN5. This is important since the parameters $\gamma$ and $c$ appear in combination in the time-of-flight analysis.

## 4. Discussion

### *4.1. The transport equation*

We wish to use the information gained in the neutron scattering experiment to interpret the anomalous temperature dependent resistivity of these nonmagnetic $RCo_2$ compounds (see section 3.1). Assuming that the scattering matrix elements are dominated by spin flip scattering processes, Boltzmann's transport equation (see e.g. [12]) offers an approximate model. The key features are as follows: the interacting, many electron system is broken into two pieces: a set of independent electron quasiparticles, which carry the electric current, and a system of dynamical spin fluctuations which are responsible for the spin flip scattering of the quasiparticles. To avoid double counting the quasiparticles are imagined to be in a conduction band (often of free electron character) whilst the spin fluctuations reside in a distinct (often of d or f character) narrow band. The influx of momentum and energy, into the spin fluctuation system, arising from the scattering processes is drained away via an immediate, unspecified, spin–lattice relaxation mechanism and hence to the thermal bath such that the spin fluctuations remain at all times in thermal equilibrium. In reality, the current carrying quasiparticles form an integral part of the spin fluctuation system and the time scales for momentum and energy transfer may not be so well separated. The model of independent current carrying quasiparticles suggests the $N$-particle distribution function may be usefully approximated by a single-particle distribution function $f(\vec{k}\sigma)$. That is, all interactions, save those due to the residual spin fluctuations, which are assumed to give the dominant temperature dependence to the resistivity, have been renormalized into the effective quasiparticles. The analysis in this article shows, that, at least in $YCo_2$ the appropriate spin fluctuation spectrum may be identified with that estimated from inelastic neutron scattering. In order to make this connection the resistivity is modelled in terms of $f(\vec{k}\sigma)$ following the Boltzmann formalism [12]. To make progress one works with a linearized Boltzmann equation and defines a new function $\Phi(\vec{k}\sigma)$:

$$f(\vec{k}\sigma) = f_0(\varepsilon_{k\sigma}) - \Phi(\vec{k}\sigma)\frac{\partial f_0(\varepsilon_{k\sigma})}{\partial \varepsilon_{k\sigma}}. \tag{7}$$

$\Phi(\vec{k}\sigma)$ is a measure of the deviation from equilibrium in the conduction electron (quasiparticle) distribution, weighted with a factor which depends on the form of the distribution. It may be regarded as the average extra energy that the (quasi-) particles have because of the transport process. The rate of change of the single-particle distribution function due to scattering is approximated by:

$$\left(\frac{\partial f}{\partial t}\right)_s = \sum_{k'\sigma'}\{P(\vec{k}'\sigma' \to \vec{k}\sigma) f(\vec{k}'\sigma')[1 - f(\vec{k}\sigma)] - P(\vec{k}\sigma \to \vec{k}'\sigma') f(\vec{k}\sigma)[1 - f(\vec{k}'\sigma')]\} \tag{8}$$

where the scattering rate (in or out of a small volume around $\vec{k}$ in phase space) has been factorized into a transition probability $P(\vec{k}\sigma \to \vec{k}'\sigma')$ and a product of initial $f(\vec{k}\sigma)$ and final state $[1 - f(\vec{k}'\sigma')]$ occupation factors. Inserting equation (7) in equation (8) and keeping terms linear in $\Phi$ equation (8) reduces to:

$$\left(\frac{\partial f}{\partial t}\right)_s = \frac{1}{k_B T}\sum_{k'\sigma'}\{P(\vec{k}\sigma \to \vec{k}'\sigma') f_0(\varepsilon_{k\sigma})[1 - f_0(\varepsilon_{k'\sigma'})][\Phi(\vec{k}'\sigma') - \Phi(\vec{k}\sigma)]\}. \tag{9}$$

From this a general expression for the resistivity may be obtained as a variational solution of the Boltzmann equation [12]:

$$\rho = \frac{1}{2k_BT}\sum_{k'\sigma',k\sigma}\{P(\vec{k}\sigma \to \vec{k}'\sigma')f_0(\varepsilon_{k\sigma})[1 - f_0(\varepsilon_{k'\sigma'})][\Phi(\vec{k}'\sigma') - \Phi(\vec{k}\sigma)]^2\}$$
$$\times\left|\sum_{k\sigma} ev_k\Phi(\vec{k}\sigma)\frac{\partial f_0(\varepsilon_{k\sigma})}{\partial\varepsilon_{k\sigma}}\right|^{-2} \tag{10}$$

where $\Phi$ plays the role of a variational function. In the simplest case the following form can be used:

$$\Phi = \vec{v}_{k\sigma}\vec{E}. \tag{11}$$

($\vec{v}_{k\sigma}$ is the drift velocity and $\vec{E}$ the electric field vector.) The transition probability $P$, in equation (10) describes the interaction between the quasiparticles (conduction electrons) and spin fluctuations. Frequently $P$ is calculated using Fermi's golden rule:

$$P(\vec{k}\sigma, i \to \vec{k}'\sigma', f) = \frac{2\pi}{\hbar}|\langle\vec{k}'\sigma', f|H_{int}|\vec{k}\sigma, i\rangle|^2\delta(\varepsilon_{k'\sigma'} + E_f - \varepsilon_{k\sigma} - E_i) \tag{12}$$

with $i$, $f$, $E_i$ and $E_f$ the initial and the final state of the spin fluctuation system and the corresponding energies and $H_{int}$ the Hamiltonian for the quasiparticle—spin fluctuation interaction. Assuming that the initial states of the spin fluctuations are in thermal equilibrium (at a given temperature $T$) equation (12) can be written as:

$$P(\vec{k}\sigma \to \vec{k}'\sigma') = \sum_i \frac{e^{-E_i/k_BT}}{Z}\sum_f P(\vec{k}\sigma, i \to \vec{k}'\sigma', f).$$

In practice the $\delta$-function in equation (12) may be of limited validity both since the scattering quasiparticles have a finite coherence time, $\tau_{qp-coh}$, and since the spin fluctuations have a finite lifetime, $\tau_{mode}$. The finite mode lifetime may significantly limit the interaction. A spin fluctuation of lifetime $\tau_{mode}$ has a contribution to the scattering weighted by approximately $e^{-\tau_{qp-coh}/\tau_{mode}}$. At low temperatures, where the thermal population factor restricts the spin fluctuation modes to low energies with lifetimes which scale like the inverse susceptibility and hence become significant (see equation (6)), the situation may be satisfactory. Under these conditions, the analogous considerations for the neutron probe (typical coherence time $10^{-12}$ to $10^{-10}$ s) indicate that the low energy spectrum of spin fluctuations as measured by neutron scattering may give a reliable estimate of the appropriate spin fluctuation spectrum for the quasiparticle scattering. However, at elevated temperatures, or for short lifetime modes in general, problems may arise. First, when $\tau_{qp-coh} \leqslant \tau_{mode} \leqslant \tau_{neutron-coh}$ the neutron probe may integrate out a sizeable portion of the spectrum and hence have a diminished sensitivity as compared to the quasiparticles. In such cases the empirical spin fluctuation spectrum as determined by neutron scattering will be a less appropriate measure of the effective spin fluctuation spectral density which drives the electrical resistivity. Second, at high temperatures, when lifetime of the average spin fluctuation is small even in comparison with the quasiparticle coherence time, $\tau_{mode} \leqslant \tau_{qp-coh}$, $\tau_{mode} \leqslant \tau_{neutron-coh}$, one may anticipate that the current carrying particles themselves will fail to see the full weight of the spin fluctuation spectral density. This may reduce the electrical resistivity due to spin fluctuation scattering $\rho_{sf}(T)$ at elevated temperatures. Parenthetically we note that the condition, $\tau_{mode} \leqslant \tau_{qp-coh}$, may also pertain in pure materials at very low temperatures especially in the presence of spin non-conservation. This would give rise to anomalous, low, resistivity. With these caveats in

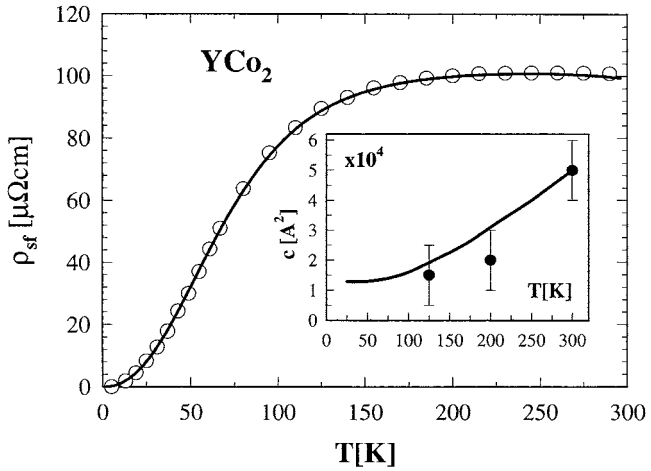


**Figure 5.** The empirical spin fluctuation contribution to the temperature dependent electrical resistivity in $YCo_2$ estimated from data presented in figure 1 after equation (2) is given by the open circles in the main frame. These data are modelled by the solid line (main frame) using a functional form of $c(T)$ which is given as the solid line in the inset to the main figure. In the inset are also given our three values of $c_{YCo_2}$ at 120, 200 and 300 K, estimated from the neutron data (see figure 3). It appears that the increase in $c$ can account for the saturation of $\rho(T)$ on heating.

mind we express the spin-flip contribution to the resistivity in terms of the dynamical spin susceptibility [13]:

$$\rho \propto \frac{1}{k_B T} \int_0^\infty \mathrm{d}\omega\, \omega n(\omega)(1 + n(\omega)) \int_{q_1}^{q_2} \mathrm{d}q\, q^3 \chi''(q, \omega) \tag{13}$$

where the sums over wavevectors in equation (10) have been transformed into integrals over the energy and momentum transfer to the spin fluctuation system. Since we consider inelastic scattering in general there is no restriction to the Fermi surface and the momentum integral runs over the available modes represented by the upper and lower limits of integration in equation (13). On account of the dispersion relation of the spin fluctuation spectrum the lower limit is a function of the energy transfer. The occupation factors have been transformed to a bosonic form via the integral relation:

$$I(\omega) = \int_{-\infty}^{\infty} \mathrm{d}\varepsilon_k f(\varepsilon_k)[1 - f(\varepsilon_k + \omega)] = \frac{\omega}{1 - \mathrm{e}^{-\beta\omega}}. \tag{14}$$

### *4.2. The calculation of the temperature dependence of the resistivity*

As discussed above, calculation of the approximate temperature dependence of the electrical resistivity is made by replacing the dynamical quasiparticle susceptibility by that determined by neutron scattering. Since the magnitude of the matrix element in the resistivity is unknown, one obtains the functional form, not the absolute value by this method. From the neutron spectra, figure 3, and the arguments given below equation (4), we have determined that the microscopic stiffness parameter $c$ is temperature dependent in the range 120 K to 300 K even if the experimental limitations of available neutron flux do not permit a very precise estimate of its value. On the other hand, over the interval, 1.5–300 K, the data for $\rho_{sf}(T)$ are rather accurate (see figure 5). Therefore we use the general formalism (equation (13)) to estimate the temperature dependence of the parameter, $c$, necessary to give the observed form of $\rho_{sf}(T)$.

In making this calculation, the absolute value of $c$ at 300 K is taken to be that determined at 300 K by both time-of-flight and neutron polarization analysis. At subsequent lower temperatures, using an iterative fitting procedure, the parameter $c$ is determined so as to reproduce $\rho_{sf}(T)$. In figure 5 we give the data, $\rho_{sf}(T)$ as the open circles and the calculated resistivity by the solid line. In the inset our three values of $c$(120 K), $c$(200 K) and $c$(300 K) estimated from the neutron data are given, and the determined functional form, $c(T)$, is represented by the solid line. It appears that the stiffening of the spectrum, i.e. the increase in $c$, may be responsible for the saturation of $\rho_{sf}(T)$ which appears typical for the $RCo_2$ compounds as illustrated in figure 1.

We now turn to the low temperature regime. As $c$ saturates at its low temperature value, the spin fluctuation contribution to the resistivity approaches quadratic behaviour (see the inset in figure 1). In this regime it is useful to calculate the enhancement of the linear term in the heat capacity attributable to the (extrapolated) dynamic spin fluctuations. Using the formalism, as developed for example in [14], for the contribution from overdamped modes to the specific heat capacity, one finds an estimated contribution between 20 and 40 mJ $mol^{-1}$ $K^{-2}$ depending on the wavevector cut-off used. This may be compared with the experimental value of 34 mJ $mol^{-1}$ $K^{-2}$ (see e.g. Yamada 1988 [15]) and supports our estimates of the magnitudes of $c$ and $\gamma$ obtained from the measured neutron spectra.

## 5. Conclusions

The spin density fluctuation spectra have been measured in the itinerant paramagnets $YCo_2$ and $ScCo_2$. The weakness of the inelastic neutron scattering signals has restricted our useful data sets to $T > 100$ K. An attempt has been made to rationalize the use of spin fluctuation spectra, as observed by inelastic neutron scattering, to calculate the temperature dependence of the resistivity. In $YCo_2$, the saturation of the resistivity may be understood as driven by the hardening of the spin fluctuation spectrum with increasing temperature. In $ScCo_2$, where the weakness of the inelastic scattering signal prohibits such a full analysis, we can only estimate that the wavevector dependent susceptibility has a magnitude of approximately 50% of that in $YCo_2$ at room temperature (figure 4 and [5]). Assuming a similar value of $\gamma$ this scales to a spin fluctuation contribution to the resistivity of approximately 50% of that in $YCo_2$. Looking at figure 1 this appears reasonable. It is to be hoped that improvements to neutron sources and advances in techniques will open up these kind of study over wider temperature intervals and allow their extension to other materials.

## Acknowledgments

We wish to thank ILL for beam time on IN5 and D7 and Professor H Nowotny (TU Vienna) for many fruitful discussions. This project has been supported by the Austrian Science Foundation under the projects P11581 and S5605. EG wishes also to express thanks for financial support from INTAS Project No 96-0630. NB thanks the ILL for support during the early stages of this work.

## References

[1] Kirchmayr H R and Poldy C 1979 *Handbook on the Physics and Chemistry of Rare Earths* vol 2, ed K A Gschneidner Jr and L Eyring (Amsterdam: North-Holland) ch 14, p 55

[2] Gratz E, Hauser R, Lindbaum A, Maikis M, Resel R, Schaudy G, Levitin R Z, Markosyan A S, Dubenko I S, Sokolov A Yu and Zochowski S W 1995 *J. Phys.: Condens. Matter* **7** 597

[3] Goto T, Sakakibara T, Murata K, Komatsu H and Fukamichi K 1990 *J. Magn. Magn. Mater.* **90/91** 700
[4] Gratz E, Resel R, Burkov A T, Bauer E and Markosyan A S 1995 *J. Phys.: Condens. Matter* **7** 6687
[5] Burzo E, Gratz E and Pop V 1993 *J. Magn. Magn. Mater.* **123** 159
[6] Gratz E 1997 *Physica* B **237/238** 470
[7] Kadowaki K and Woods S 1986 *Solid State Commun.* **58** 507
[8] Pelleg J and Carlson O N 1965 *J. Less-Common Met.* **9** 281
[9] Bernhoeft N R and Lonzarich G G 1995 *J. Phys.: Condens. Matter* **7** 7325
[10] Lonzarich G G and Taillefer L 1985 *J. Phys. C: Solid State Phys.* **18** 4339
[11] Moria T 1985 *Spin Fluctuations in Itinerant Electron Magnetism* (Berlin: Springer)
[12] Ziman J M 1960 *Electrons and Phonons* (Oxford: Clarendon) p 283
[13] Ueda T and Moriya T 1975 *J. Phys. Soc. Japan* **39** 605
[14] Edwards D M and D Lonzarich G G 1992 *Phil. Mag.* B **65** 1185
[15] Yamada H 1988 *Physica* B **149** 390